J. At. Mol. Sci.
doi: 10.4208/jams.032714.062614a

Vol. **5**, No. 3, pp. 254-262
August 2014

# Optical limiting and dynamical two-photon absorption for femtosecond laser pulses in BDBAS

Yu-Jin Zhang, Yong Zhou*, Jun-Yang Ma, Yao Chen, and Chuan-Kui Wang

*College of Physics and Electronics, Shandong Normal University, Jinan 250014, China*

Received 27 March 2014; Accepted (in revised version) 26 June 2014
Published Online 8 August 2014

**Abstract.** By numerically solving the Maxwell-Bloch equations using an iterative predictor-corrector finite-difference time-domain (FDTD) technique, the optical limiting (OL) and two-photon absorption (TPA) properties for femtosecond laser pulses in a strong TPA organic molecular (4,4′-bis (di-*n*-butylamino) stilbene (BDBAS)) medium are studied. The medium has obvious OL behavior in a certain intensity region which is dependent on the propagation distance, sample concentration, input pulse width and effect of optical ionization. Moreover, dynamical TPA cross sections are obtained, showing an increasing trend with the broadening of the pulse width and the propagation distance in the femtosecond time domain.

**PACS**: 33.80.-b, 82.50.Pt, 31.15.A-
**Key words**: optical limiting, two-photon absorption, organic molecule

## 1 Introduction

The interaction between light and matter has always been evoking one's curiosity and motivation [1-4]. On the basis of the advances in ultra-short and ultra-intense laser technology, it is available to generate extremely short and intense pulses [5,6], which pushes the nonlinear optics into a new stage [7-9]. In recent years, studies of OL have been more and more interesting due to the need for protection of the optical sensors against intense laser radiation and for peak-power stabilization of the intense laser pulses [10-12]. One of the key challenges in the development of optical limiters is to search for appropriate materials that rapidly respond to the applied laser intensity, own good nonlinear absorption characteristics over a broad range of wavelengths, and have a high damage threshold. With the progress of design and synthesis technology of organic materials, organic

*Corresponding author. *Email address:* zhangyujin312@163.com (Y. Zhou)

 

conjugated compounds have shown great promise for OL applications [10,13-15]. They possess various nonlinear mechanisms to produce OL, in which TPA is the major one.

As a typical organic conjugated compound, BDBAS were demonstrated to have obvious nonlinear optical properties [16]. In this work, taking BDBAS as the sample, we numerically study the dynamical behavior of OL caused by TPA and determine the dynamical TPA cross section when ultra-short laser pulses are used. Also, the influences of propagation distance, sample concentration, effect of optical ionization and pulse width on OL are discussed.

## 2 Theoretical methods

### 2.1 Maxwell-Bloch equations for a three-level system

Based on the semi-classical theory on the interaction between laser pulses and molecules, the electromagnetic radiation can be described classically by Maxwell equations, and the molecular system can be treated by Bloch equations quantum mechanically.

We assume that the incident electromagnetic field is polarized along the x-axis and propagates along the z-axis to an input interface of the medium at $z$=0. Then the Maxwell equations can take the form as follows:

$$\begin{aligned}\frac{\partial E_x}{\partial z} &= -\mu_0 \frac{\partial H_y}{\partial t} \\ \frac{\partial H_y}{\partial z} &= -\frac{\partial P_x}{\partial t} - \varepsilon_0 \frac{\partial E_x}{\partial t}\end{aligned} \tag{1}$$

where $\mu_0$ and $\varepsilon_0$ are the permeability and permittivity of free space, respectively.

Taken the relaxation effect and ionization effect into consideration, the density matrix equation can be written as:

$$\begin{aligned}\dot{\rho}_{mn} &= -\frac{i}{\hbar}[\hat{H},\hat{\rho}]_{mn} - \gamma_{mn}\rho_{mn} - \frac{\gamma_{ph}^{(m)}(t)+\gamma_{ph}^{(n)}(t)}{2}\rho_{mn} \qquad (m \neq n) \\ \dot{\rho}_{nn} &= -\frac{i}{\hbar}[\hat{H},\hat{\rho}]_{nn} + \sum_{E_m > E_n} \Gamma_{nm}\rho_{mm} - \sum_{E_m < E_n} \Gamma_{mn}\rho_{nn} - \gamma_{ph}^{(n)}(t)\rho_{nn}\end{aligned} \tag{2}$$

here $\Gamma_{nm}$ gives decay rate of the population from level $m$ to level $n$, and $\gamma_{mn}$ is the relaxation rate of the density matrix element $\rho_{mn}$·$\gamma_{ph}^{(m)}(t)$ and $\gamma_{ph}^{(n)}(t)$ are the ionization rate of level $m$ and level $n$, respectively. It can be expressed as $\gamma_{ph}^{(i)}(t) = \sigma_i I(t)/(\hbar\omega_p)$, where $I(t) = c\varepsilon_0 \mid E(t,z) \mid^2/2$ is the laser intensity, $\sigma_i$ is the ionization cross section of level $i$, which has an order about $10^{-20}$ m$^2$ [17], and $\omega_p$ is the frequency of the input pulse. $\hat{H}$ is the Hamiltonian of the system, which can be expressed as the sum of free Hamiltonian and interaction Hamiltonian. Within the dipole approximation, it can be written as:

$$\hat{H} = \hat{H}_0 + \hat{H}' = \hat{H}_0 - \hat{\mu}\cdot E. \tag{3}$$

Taking a three-level system as the example, and supposing ionization only take place on the highest level, i.e., $\gamma_{ph}^{(0)}(t)=\gamma_{ph}^{(1)}(t)=0$, by setting up the relations $\rho_{01}=\frac{u_0+iv_0}{2}$, $\rho_{12}=\frac{u_1+iv_1}{2}$, $\rho_{02}=\frac{u_2+iv_2}{2}$, we get the Bloch equations for the three-level system as follows,

$$
\begin{aligned}
&\frac{\partial u_0}{\partial t}=-\omega_{10}v_0+\frac{E\cdot(\mu_{11}-\mu_{00})}{\hbar}v_0+\frac{E}{\hbar}\cdot(\mu_{12}v_2+\mu_{02}v_1)-\gamma_{01}u_0\\
&\frac{\partial v_0}{\partial t}=\omega_{10}u_0-\frac{E\cdot(\mu_{11}-\mu_{00})}{\hbar}u_0-\frac{E\cdot(\mu_{12}u_2-\mu_{02}u_1)}{\hbar}-\frac{2}{\hbar}E\cdot\mu_{01}(\rho_{00}-\rho_{11})-\gamma_{01}v_0\\
&\frac{\partial u_1}{\partial t}=-\omega_{21}v_1+\frac{E\cdot(\mu_{22}-\mu_{11})v_1}{\hbar}-\frac{E\cdot(\mu_{02}v_0+\mu_{01}v_2)}{\hbar}-\gamma_{12}u_1-\frac{\gamma_{ph}^{(2)}(t)}{2}u_1\\
&\frac{\partial v_1}{\partial t}=\omega_{21}u_1-\frac{E\cdot(\mu_{22}-\mu_{11})}{\hbar}u_1-\frac{E\cdot(\mu_{02}u_0-\mu_{01}u_2)}{\hbar}-\frac{2}{\hbar}E\cdot\mu_{12}(\rho_{11}-\rho_{22})-\gamma_{12}v_1-\frac{\gamma_{ph}^{(2)}(t)}{2}v_1\\
&\frac{\partial u_2}{\partial t}=-\omega_{20}v_2+\frac{E\cdot(\mu_{22}-\mu_{00})}{\hbar}v_2+\frac{E\cdot(\mu_{12}v_0-\mu_{01}v_1)}{\hbar}-\gamma_{02}u_2-\frac{\gamma_{ph}^{(2)}(t)}{2}u_2\\
&\frac{\partial v_2}{\partial t}=\omega_{20}u_2-\frac{E\cdot(\mu_{22}-\mu_{00})}{\hbar}u_2-\frac{E\cdot(\mu_{12}u_0-\mu_{01}u_1)}{\hbar}-\frac{2}{\hbar}E\cdot\mu_{02}(\rho_{00}-\rho_{22})-\gamma_{02}v_2-\frac{\gamma_{ph}^{(2)}(t)}{2}v_2\\
&\frac{\partial\rho_{00}}{\partial t}=\frac{E\cdot(\mu_{01}v_0+\mu_{02}v_2)}{\hbar}+\Gamma_{01}\rho_{11}+\Gamma_{02}\rho_{22}\\
&\frac{\partial\rho_{11}}{\partial t}=-\frac{E\cdot(\mu_{01}v_0-\mu_{12}v_1)}{\hbar}+\Gamma_{12}\rho_{22}-\Gamma_{01}\rho_{11}\\
&\frac{\partial\rho_{22}}{\partial t}=-\frac{E\cdot(\mu_{02}v_2+\mu_{12}v_1)}{\hbar}-\Gamma_{02}\rho_{22}-\Gamma_{12}\rho_{22}-\gamma_{ph}^{(2)}(t)\rho_{22}
\end{aligned}
\tag{4}
$$

where $\mu_{mn}=\mu_{nm}(m,n=0,1,2)$ are the permanent electric dipole moments ($m=n$) or the transition electric dipole moments ($m\neq n$) of the molecule, and $\hbar\omega_{mn}$ is the excitation energy between the states $m$ and $n$.

We can couple the Maxwell and the Bloch equations to each other by the macroscopic polarization $P_x$:

$$
\begin{aligned}
\frac{\partial P_x}{\partial t}&=\frac{\partial(N\langle\hat{\mu}_x\rangle)}{\partial t}=\frac{\partial\big(Ntr(\hat{\mu}_x\hat{\rho})\big)}{\partial t}\\
&=N(\mu_{00x}\dot{\rho}_{00}+\mu_{11x}\dot{\rho}_{11}+\mu_{22x}\dot{\rho}_{22}+\mu_{01x}\dot{u}_0+\mu_{12x}\dot{u}_1+\mu_{02x}\dot{u}_2)\\
&=N[(\mu_{00x}-\mu_{11x})\Gamma_{01}\rho_{11}-(\mu_{22x}-\mu_{00x})\Gamma_{02}\rho_{22}\\
&\quad-(\mu_{22x}-\mu_{11x})\Gamma_{12}\rho_{22}-\mu_{22x}\gamma_{ph}^{(2)}(t)\rho_{22}-\mu_{01x}(\omega_{10}v_0+\gamma_{01}u_0)\\
&\quad-\mu_{12x}(\omega_{21}v_1+\gamma_{12}u_1+\frac{\gamma_{ph}^{(2)}(t)}{2}u_1)-\mu_{02x}(\omega_{20}v_2+\gamma_{02}u_2+\frac{\gamma_{ph}^{(2)}(t)}{2}u_2)]
\end{aligned}
\tag{5}
$$

where $N$ is the molecular density.

### 2.2 Formula for the dynamical TPA cross section

The static TPA cross section of molecules can be theoretically calculated on the basis of quantum approaches set on *ab initio* level. But those approaches neglect the interaction between laser and compounds, which leads to discrepancy from the experiment value. Here we introduce a way to investigate the dynamical TPA cross section.

The differential equation that describes pulse propagation in the presence of one and two-photon absorption but in the absence of significant recombination, diffusion, and thermal runaway can be written as [13]

$$dI/dz+\alpha I+\beta I^2=0 \tag{6}$$

where $\alpha$ denotes the linear absorption coefficient and $\beta$ is the TPA coefficient.

The analytical solution of eq. (6) is

$$I_z=\frac{\alpha I_0\exp(-\alpha z)}{\alpha+\beta I_0\left(1-\exp(-\alpha z)\right)} \tag{7}$$

Assuming $\beta=\beta_0+\xi I_0$ [18], it can be re-formed as follows:

$$\frac{1}{T}=\frac{I_0}{I_z}=\exp(\alpha z)+\frac{[\exp(\alpha z)-1]\beta_0}{\alpha}I_0+\frac{\xi[\exp(\alpha z)-1]}{\alpha}I_0^2 \tag{8}$$

where $T$ is the intensity transmission at the propagation distance of $z$. One can calculate the values of $\alpha$ and $\beta_0$ by nonlinear fitting of eq. (8). The molecular TPA cross section $\sigma_{tp}$ is related to $\beta_0$ by

$$h\nu\beta_0=\sigma_{tp}N \tag{9}$$

where $h\nu$ is the input photon energy.

## 3 Results and discussion

The structure of BDBAS is shown in Fig. 1. Electronic structure calculations show that the molecule has only one charge-transfer state (the first excited state $S_1$) that dominates the maximum one-photon absorption in the optical region. The strongest TPA occurs on the fourth excited state $S_2$ . To describe the nonlinear optical response of this molecule under a visible light, a three-level model including the ground state $S_0$, the charge-transfer state $S_1$ and the fourth excited state $S_2$ is thus needed. Time-dependent DFT/B3LYP method implemented in DALTON package [19] is employed to obtain the transition dipole moments and the excitation energies of the molecule. The 6-31G basis set is chosen for all computations. Numerical results show that the transition dipole moments between $S_0$ and $S_1$ and between $S_1$ and $S_2$ states are, $\mu_{01}=3.747\times10^{-29}$ C·m and $\mu_{12}=4.154\times10^{-29}$ C·m, respectively, while the transition dipole moments among other states in the low

energy region are nearly zero. The permanent dipole moments of all states are approximately equal to zero due to the one-dimensional symmetrical characteristic of the molecule. The excitation energies of $S_1$ and $S_2$ states, are 3.41 eV and 4.20 eV, respectively. To demonstrate the OL behavior induced by TPA, the frequency of the incident field is taken to be half of the frequency between the $S_2$ and $S_0$ states $\omega_p = \omega_{20}/2$. Considering the ionization effect, we should take the ionic states into account. The energy difference between the ionic ground state and the ground state is 5.26 eV. While the energy of the incident photon is 2.10 eV, the ionization of the ground state is impossible. Besides, due to the fact that the population of $S_1$ state is rather small during TPA process, the ionization of the $S_1$ state can be neglected. The energy difference between the $S_2$ state and the ionic ground state is 1.06 eV, which is smaller than the energy of the incident photon. As a result, the $S_2$ state has a possibility to occur single photon non-resonant ionization followed by the TPA process.

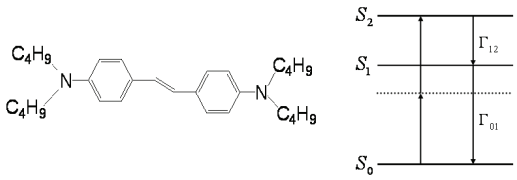


Figure 1: Scheme of molecular structures (left) and transitions (right) of BDBAS.

We choose the initial field with a hyperbolic secant shape defined as $E_x(z,t=0) = F_0 \mathrm{sec}h[1.76(z/c+z_0/c)/\tau]\cos\lfloor\omega_p(z+z_0)/c\rfloor$. Here $F_0$ is the peak amplitude of the input electric field, and $\tau$ is the full width at half maximum (FWHM) of the pulse intensity envelope. The choice of $z_0$ ensures that the pulse penetrates negligibly into the medium at $t$=0. The decay rates of excited states $\Gamma_{01}$, $\Gamma_{12}$ and $\Gamma_{02}$ are equal to $1.0\times10^9$/s, $1.0\times10^{12}$/s and 0 [20], respectively. The molecule is assumed to be rest in its ground state before the light is turned on, i.e., $\rho_{00}(t=0)=1$, $\rho_{11}(t=0)=\rho_{22}(t=0)=0$.

## 3.1 Optical limiting

### 3.1.1 Without the consideration of ionization

Fig. 2 gives the output fluence $S_{out}$ as a function of the input fluence $S_{in}$. The role of the sample thickness is shown in Fig. 2(a). One can clearly see that for certain input fluence, the output fluence decreases rapidly during pulse propagation, which means the OL performance is much better for a longer distance than that for shorter distance. The main mechanism is that during the pulse propagation, more energy is transferred from the field into the medium due to the interaction. Fig. 2(b) shows the influence of the sample density on the OL behavior. As can be seen, larger concentration results in stronger OL behavior at the same distance. This is because with the number of particle increases, the nonlinear absorption becomes stronger, which leads to the pulse energy

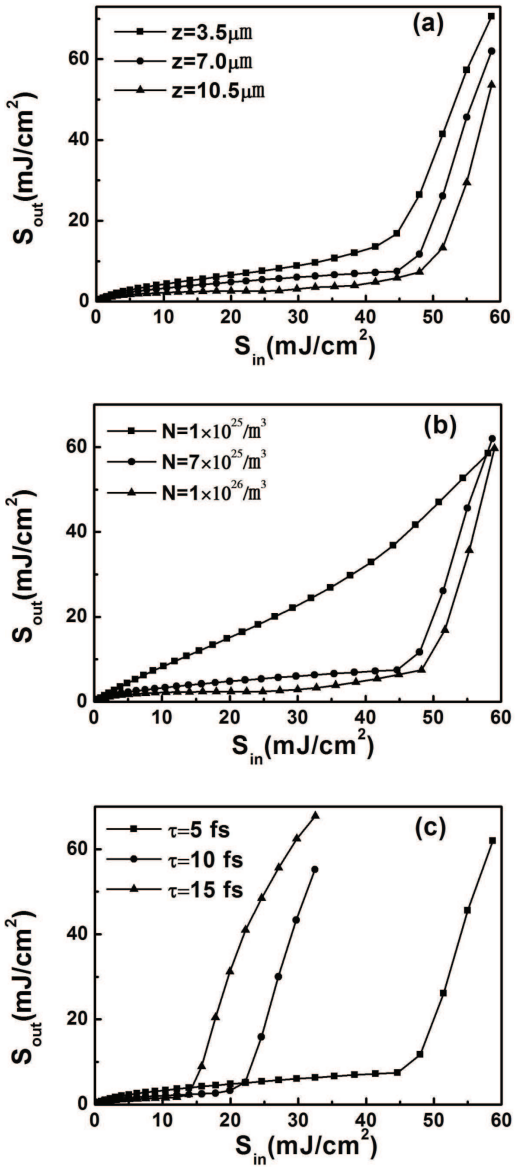


Figure 2: Output fluence $S_{out}$ versus input fluence $S_{in}$. (a) $N=7\times10^{25}/\mathrm{m}^3$, $\sigma_i$=0, $\tau=5$ fs. (b) $z=7.0$ $\mu$m, $\sigma_i=0$, $\tau=5$ fs. (c) $z=7.0$ $\mu$m, $N=7\times10^{25}/\mathrm{m}^3$, $\sigma_i=0$.

transmittance decreases, and then resulting in more obvious OL. Thus, one can improve the OL of the medium by increasing the length or concentration of the absorber.

The duration of the input pulse plays a key role in the nonlinear absorption process. Fig. 2(c) displays the $S_{out}/S_{in}$ curves for different input pulse widths. The OL behavior and its breakdown can be clearly seen. On one hand, the OL window for longer pulse is narrower than that of the shorter pulse, which corresponds well with our study pre-

viously [21]. Therefore, shorten the width of pulse can efficiently enhance the threshold. On the other hand, the saturation value of output fluence is much smaller for longer pulse. This is because with the same fluence, shorter duration leads to shorter interacted time and weaker absorption of the medium compared with longer pulse, which means higher output fluence. All in all, through our simulation, we can see that the shorter pulse favors the OL behavior for a broader dynamical OL range, while it has a higher output saturation value.

### 3.1.2 With the consideration of ionization

In order to elucidate the influence of the ionization effect on the OL behavior, the $S_{out}/S_{in}$ curves for different ionization cross sections at the propagation distance of 7.0 $\mu$m are shown in Fig. 3. It is evident that without the consideration of ionization, the OL behavior breaks down when the input laser fluence increases to 46 mJ/cm$^2$. While taking the ionization into consideration and the ionization cross section $\sigma_i \leq 1\times10^{-20}$ m$^2$, the breakdown of OL turns weak. This is because the ionization rate increases as the input laser fluence enlarges, which leads to the reduction of output fluence, i.e., the ionization favors the OL behavior for its broader OL window. But when the ionization cross section reaches $5\times10^{-20}$ m$^2$, the situation becomes different - the OL behavior is obviously weaken. The main mechanism is that with the increase of ionization cross section, more and more particles are ionized, which makes the nonlinear interaction between laser and medium weaker.

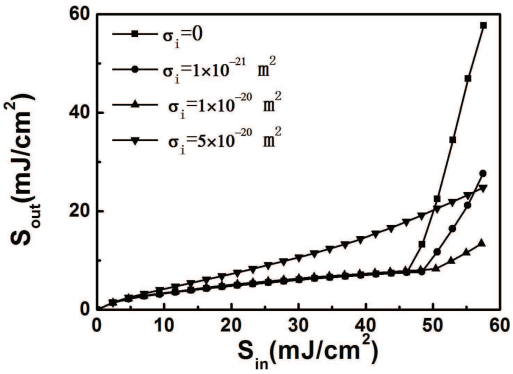


Figure 3: Output fluence $S_{out}$ versus input fluence $S_{in}$ with different ionization cross section. $z=7.0$ $\mu$m, $N=7\times10^{25}$/m$^3$, $\tau=5$ fs.

## 3.2 Calculation of the dynamical TPA cross section

Using the input-output peak-intensity relation in the OL region obtained by solving Maxwell-Bloch equations, we get the dynamical TPA cross sections [21] of this organic molecule. The dynamical values of TPA cross section are obtained as 758.9 GM, 1843.6 GM, and 2783.4 GM (1GM=$1\times10^{-50}$cm$^4$s/photon) for pulse widths of 5 fs, 10 fs, and 15 fs

at the propagation distance of 7.0 $\mu$m, respectively. These values are of the same order of magnitude with the static TPA cross section $\sigma_{tp}$=1430 GM, which illustrates that one-step resonant TPA mainly occurs in the femtosecond time domain. Besides, Ehrlich *et al.* measured the TPA cross section of BDBAS by direct nonlinear optical transmission on open Z-scan technique [16]. Compared with their experiment result $\sigma_{tp}$=9300 GM, our calculated result is on the same order of magnitude but somewhat smaller. The discrepancy mainly results from that the experiment was taken under the condition of laser with the pulse duration of 5 ns and wavelength of 600 nm in which two-step TPA process takes place.

From the above calculation, one can expect that the TPA cross section is an increasing function of the pulse width. For added clarification, Fig. 4 shows the dependence of TPA cross sections on the pulse widths and propagation distances. One can see that $\sigma_{tp}$ increases almost linearly with the broadening of the input pulse, which coincides well with the relationship between the TPA cross section and the pulse duration for short pulses in [22]. The mechanism is that with a broader pulse width, the interaction between the field and the medium stays longer which leads to stronger absorption. Furthermore, propagation distance also plays an important role on the TPA cross section, and enhancing dependence of TPA cross section on propagation distance is observed. Therefore, thickness of the molecular sample should be taken into account when comparing the TPA cross sections of different samples by different measurements.

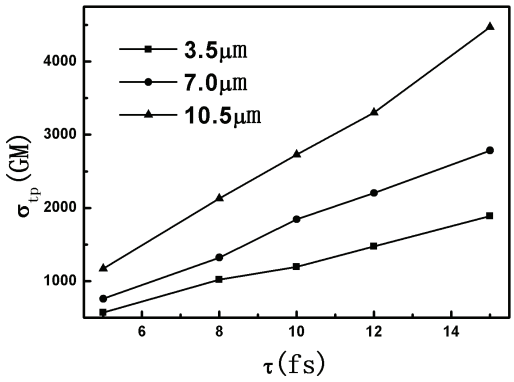


Figure 4: Dependence of TPA cross section $\sigma_{tp}$ on pulse width $\tau$ and propagation distances.

## 4 Conclusions

We provide a dynamical analysis of OL for the ultra-short laser pulses propagating in a strong TPA organic molecular medium BDBAS by solving the Maxwell-Bloch equations using an iterative predictor-corrector FDTD method. Dependences of OL on the propagation distance, sample concentration, and input pulse width as well as effect of optical ionization are observed. The dynamical TPA cross section $\sigma_{tp}$ is calculated by numerical

fitting, which is almost a linearly increasing function of the pulse width in femtosecond time domain. Our results indicate that when measuring the TPA cross section, one should take the input pulse width, the density and thickness of the molecular samples into consideration.

**Acknowledgments.** This work was supported by the 973 program under Grant No. 2011CB808105. Partial computation is carried on the HPC supported by CETV and guoshi.com.

**References**

[1] B. Liang, K. N. Jia, Y. Liang, D. M. Tong, and X. J. Fan, Chinese J. Comput. Phys. 28 (2011) 583 (in Chinese).
[2] K. Zhao, H. Y. Li, J. C. Liu, and C. K. Wang, Chinese Phys. 15 (2006) 2338.
[3] Y. Zhou, Q. Miao, and C. K. Wang, Chinese Phys. B 20 (2011) 044205.
[4] H. Y. Li, K. Zhao, R. Q. Pan, Y. H. Sun, and C. K. Wang, Acta Phys. Sin. Ch. Ed. 54 (2005) 2072 (in Chinese).
[5] L. J. Kong, L. M. Zhao, S. Lefrancois, D. G. Ouzounov, C. X. Yang, and F. W. Wise, Opt. Lett. 37 (2012) 253.
[6] H. Vincenti and F. Qu*éré*, Phys. Rev. Lett. 108 (2012) 113904.
[7] Z. B. Liu and X. J. Fan, Chinese J. Comput. Phys. 29 (2012) 881.
[8] H. J. Ding, J. Sun, Y. J. Zhang, and C. K. Wang, J. At. Mol. Sci. 4 (2013) 349.
[9] Y. J. Zhang, Y. Z. Song, and C. K. Wang, J. At. Mol. Sci. 5 (2014) 163.
[10] L. W. Tutt, and T. F. Boggess, Prog. Quant. Electron. 17 (1993) 299.
[11] S. Hughes and B. Wherrett, Phys. Rev. A 54 (1996) 3546.
[12] S. Kim, D. McLaughlin, and M. Potasek, Phys. Rev. A 61 (2000) 025801.
[13] J. D. Bhawalkar, G. S. He, and P. N. Prasad, Rep. Prog. Phys. 59 (1996) 1041.
[14] S. Gavrilyuk, J. C. Liu, K. Kamada, H. Ågren, and F. Gel'mukhanov, J. Chem. Phys. 130 (2009) 054114.
[15] H. S. Nalwa and S. Miyata, Opt. Eng. 36 (1997) 2622.
[16] J. E. Ehrlich, X. L. Wu, I. Y. S. Lee, Z. Y. Hu, H. R*ö*ckel, S. R. Marder, and J. W. Perry, Opt. Lett. 22 (1997) 1843.
[17] R. Buffa, M. P. Anscombe, and J. P. Marangos, Phys. Rev. A 67 (2003) 033801.
[18] G. S. He, Q. D. Zheng, A. Baev, and P. N. Prasad, J. Appl. Phys. 101 (2007) 083108.
[19] DALTON, a molecular electronic structure program, Release Dalton2013 (2013), see http://dalton program.org/.
[20] S. Gavrilyuk, S. Polyutov, P. C. Jha, Z. Rinkevicius, H. Ågren, and F. Gel'mukhanov, J. Phys. Chem. A 111 (2007) 11961.
[21] C. K. Wang, J. C. Liu, K. Zhao, Y. P. Sun, and Y. Luo, J. Opt. Soc. Am. B 24 (2007) 2436.
[22] F. Gel'mukhanov, A. Baev, P. Mac*á*k, Y. Luo, and H. Ågren, J. Opt. Soc. Am. B 19 (2002) 937.